International Journal of Aquatic Science
ISSN: 2008-8019
Vol 12, Issue 03, 2021

A Study On Carbon Storage At Cuddalore District In Tamil Nadu Using Geospatial Techniques

R. Ramasubbu[1], S. Palanivelraja[2]

[1]*Research Scholar, Department of Civil Engineering, Annamalai University*
[2]*Professor, Department of Civil Engineering, Annamalai University*

Abstract:India is a developing country with an increasing rate of economic growth. Meanwhile, it is seen that the carbon footprint is increasing. If carbon cannot be sequestered, it is released into the atmosphere, increasing carbon footprints. Carbon was typically sequestered in the biomass of vegetation and soil in the form of soil organic matter. Cuddalore district is a significant district in Tamil Nadu. The district is in the state's Eastern Coastal Region. Natural hazards such as cyclones frequently strike this territory, causing changes in the vegetation and, consequently, the land use pattern. This affects the amount of carbon sequestered in this environment. The land use pattern in the Cuddalore district is shifting due to natural dangers and unnatural causes. The district is growing at a breakneck pace. As a result, it is critical to research carbon sequestration. The impact of land-use changes on the carbon sequestered in this area will be explored using geospatial techniques in this study work. The various land uses in this area have been categorised using GIS values for the Normalised Difference Vegetation Index (NDVI). Carbon can be sequestered in four carbon pools in each classed land use: above-ground biomass, below-ground biomass, soil organic matter, and dead organic matter. Soil organic matter is the most significant carbon sink among the four-carbon pools. Using field data, the allometric equations estimated the various carbon reservoirs (soil bulk density, tree diameter at breast height, diameter, and height of deadwood).

Keywords: CO_2 Storage, Remote Sensing, NDVI, Land Use , Land Cover

1. INTRODUCTION

Carbon is found in every living organism and is the primary component of life on Earth. Carbon exists in various forms, the most prevalent of which are plant biomass, soil organic matter, and the gas carbon dioxide (CO2) in the atmosphere and seas (Horwath, 2007). Carbon emissions come from various sources, and carbon is a contributing component to global warming, which is the world's most feared threat. Over the last century, human activities such as the combustion of fossil fuels, deforestation, and urbanisation have increased the atmospheric concentration of CO2 and other greenhouse gases (Giri and Madla, 2017). When plants absorb carbon dioxide as part of the biological carbon cycle, it is removed from the atmosphere (or "Sequestered") (Peterson and Hustrulid, 1998). Carbon Sequestration is the act of transferring and securely storing atmospheric CO2 into other long-lived carbon reservoirs that would have been vented or remained in the atmosphere otherwise (Orr, 2004). Remote sensing data is a cost-effective method of calculating the biomass and ultimately carbon sequestration value of plants across a vast region in a short period (Tripathi *et al.*, 2010). Conventional approaches such as remotely

sensed satellite data and geographic information systems (GIS) are used to quantify the quantity of carbon sequestered in above-ground biomass over a broader area. The study examines carbon sequestration at the macro and micro levels for each land use and land cover type in the Cuddalore district. The LULC gradually alters throughout time to meet the demands of an ever-growing population. Changes in LULC influence carbon sequestration. Remote sensing, and GIS software will be used to examine the change in LULC. The amount of biomass on the vegetation varies according to its density. Carbon sequestered by each LULC will be computed using an allometric equation.

objectives of the study:

1. To gather the digital geological data from the Geological Survey of India (GSI) for the study area.
2. To extract the Land Use and Land Cover LULC data from Landsat satellite.
3. To create a Land Use Land Cover LULC map from satellite imagery using NDVI
4. To compute areas from the LULC map.
5. To estimate the carbon sequestration by using allometric equations.

2. STUDY AREA

Cuddalore district covers 3,564 square kilometres. Villupuram District flanks it on the north, the Bay of Bengal on the east, Nagapattinam District on the south, and Perambalur District on the west. The district is drained in the north by the Gadilam and Pennaiyar rivers, and in the south, the Vellar and Kollidam rivers (Coleroon). The district's general geographical area is 3678 square kilometres, with a 68-kilometre-long coastal line extending from Puducherry Union Territory in the north to the mouth of the River Coleroon in the south. Figure 1 shows the location map of the study area.

International Journal of Aquatic Science
ISSN: 2008-8019
Vol 12, Issue 03, 2021

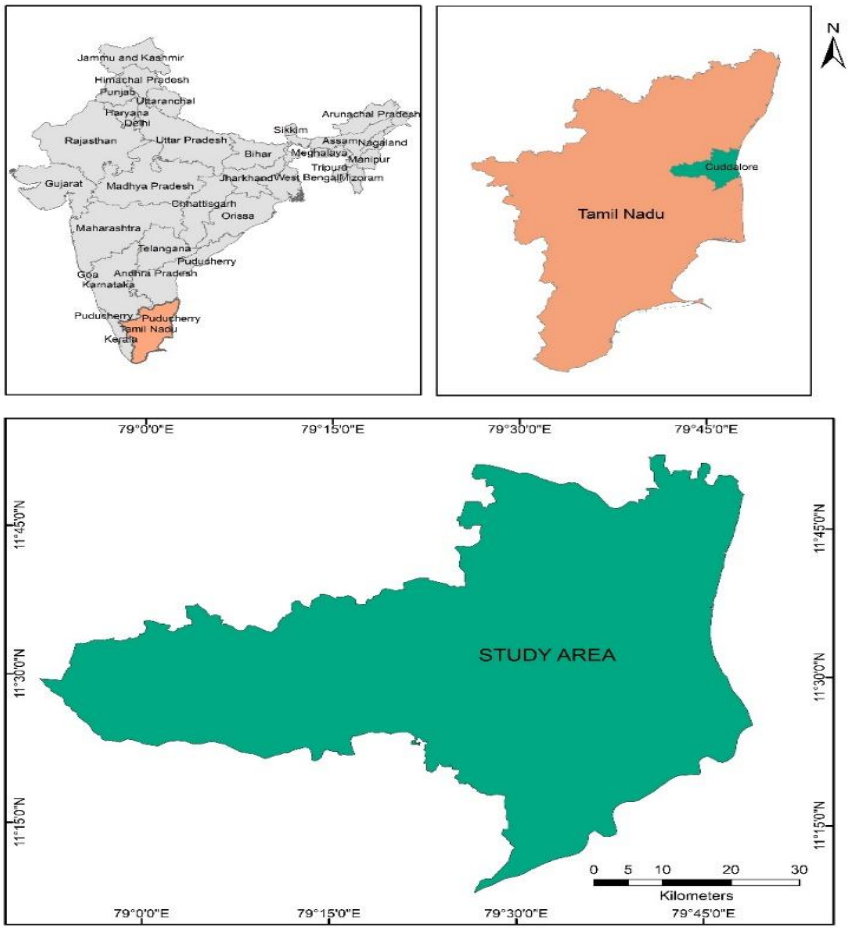

Figure 1 Location map of the study area

3. METHODOLOGY

Remote sensing technology enables the capture and analysis of georeferenced data from various platforms and can be operationally linked to spatial data layers and models included within a GIS. The ease with which Remote sensing data may be integrated with other sources of information makes geospatial technology one of the most potent contemporary instruments (Köhl, Magnussen and Marchetti, 2006). Geographic information systems (GIS) collect and pre-process spatial data from a variety of sources. It includes utilities for managing attribute data, location information, and topology in spatial analysis. Remote sensing data can be utilised as an input to a GIS for analysis. GIS can provide auxiliary data that can enhance Remote sensing analysis to discriminate between ecosystem kinds, land cover types, and land use classifications. Remote sensing and other spatial data integrated into a GIS enable modelling and scenario analysis. Integrated remote sensing and geographic information systems (GIS) can be used as a Decision Support System (DSS) to manage and monitor carbon sequestration (Giri and Madla, 2017).

The study is required to calculate the amount of carbon sequestrated per unit area in four pools, i.e., above-ground biomass (abg), below-ground biomass (bgb), soil organic matter (som) and dead organic matter (dom). For the requirements, the fieldwork has been carried out along with the Remote sensing. Using the field data, the quantity of carbon in each pool for each land use is estimated based on an allometric equation (Djomo *et al.*, 2010). The diameter of trees at

breast height (DBH) is measured from the few samples within a plot to calculate the carbon pool quantity above and below-ground biomass. The amount of carbon present in soil organic matter has been estimated by collecting soil samples randomly throughout the study area. The diameter and height of deadwood of the trees are measured to calculate the carbon quantity from dead organic matter.

This study includes the remote sensing method to identify carbon sequestration in the Cuddalore district. In remote sensing, Land use and Landcover patterns of the study area have been identified along with the NDVI (Normalized Difference Vegetation Index).

This study used Landsat 8 OLI (Operational Land Imager) data to identify LULC and NDVI patterns of the district. Landsat 8 data has a spectral resolution of coastal aerosol, visible region, NIR, SWIR, panchromatic, and TIRS. Bands 6 and 9 have a spatial resolution of 30m, band 7 has a spatial resolution of 60m, band 8 has a spatial resolution of 15m, and band 10 and 11 have a spatial resolution of 100m. The temporal resolution is 16 days for the Landsat 8 OLI satellite.

Initially, noise reduction was performed on the satellite data using the median filter method. The satellite images were then geometrically corrected and georeferenced using the UTM 43N projection. Additionally, the data were resampled using the nearest neighbour technique. The images with a resolution of 15m were created by combining the PAN (eighth band) and MS (Multi-Spectral) bands. This technique is also known as pansharpening (Aiazzi *et al.*, 2009). Pansharpening was performed because the Landsat series pictures have a low spatial resolution (30 m) than the MS image (Liu, 2000; Pardo-Pascual *et al.*, 2012; Aran Castro A J *et al.*, 2021). The data become high resolution upon pan-sharpening.

After the Pan sharpening, the LULC classification was performed. LULC classification was carried out using the maximum likelihood classifier (Settle and Briggs, 1987). The Normalised Difference Vegetation Index (NDVI) was also adopted in the study because it has been the commonly used vegetation index (Kriegler *et al.*, 1969). The NDVI classification clearly distinguishes vegetation from other land coverings (Pagare N S *et al.*, 2021). This index ranges from -1 to 1. It is computed as follows:

NDVI = NIR-red / NIR-red

4. RESULTS AND DISCUSSION

NDVI was mapped for 2015, 2018 and 2020 using the Landsat 8 data (Figure 2.3,4). The dense vegetation canopy tends to have positive values (0.3 to 0.8) of NDVI. The data set were taken in the summer period to avoid the clouds. Hence the values were too low, and the district had a low, dense vegetation canopy during the summer period. Water bodies (e.g., lakes and rivers) had a relatively low reflectance in both spectral bands (at least away from shores), and hence, it results in very low positive or even slightly negative NDVI values. The district has some major rivers and lakes, including the Coleroon river and the Veeranam lake. Soils generally exhibit a 29 near-infrared spectral reflectance somewhat more significant than the red, and thus it tends to generate small positive NDVI values (0.1 to 0.2). Very low values of NDVI (0.1 and below) correspond to barren areas of rock, sand. Moderate values represent shrub and grassland (0.2 to 0.3).

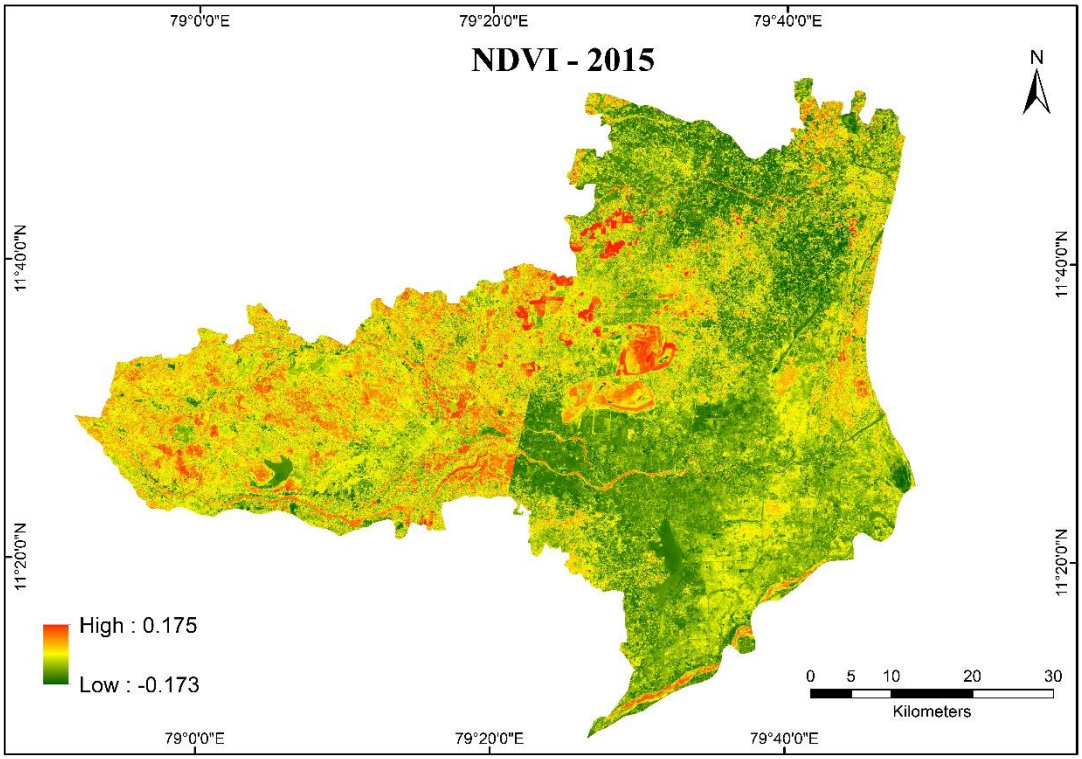

Figure 2 NDVI for the year 2015

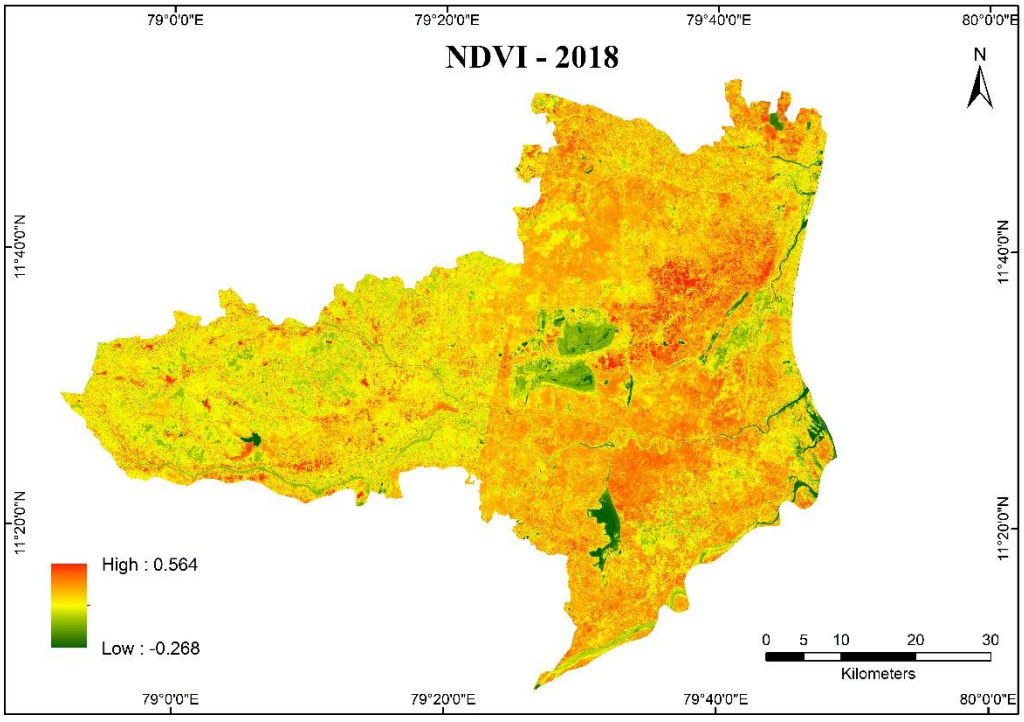

Figure 3 NDVI for the year 2018

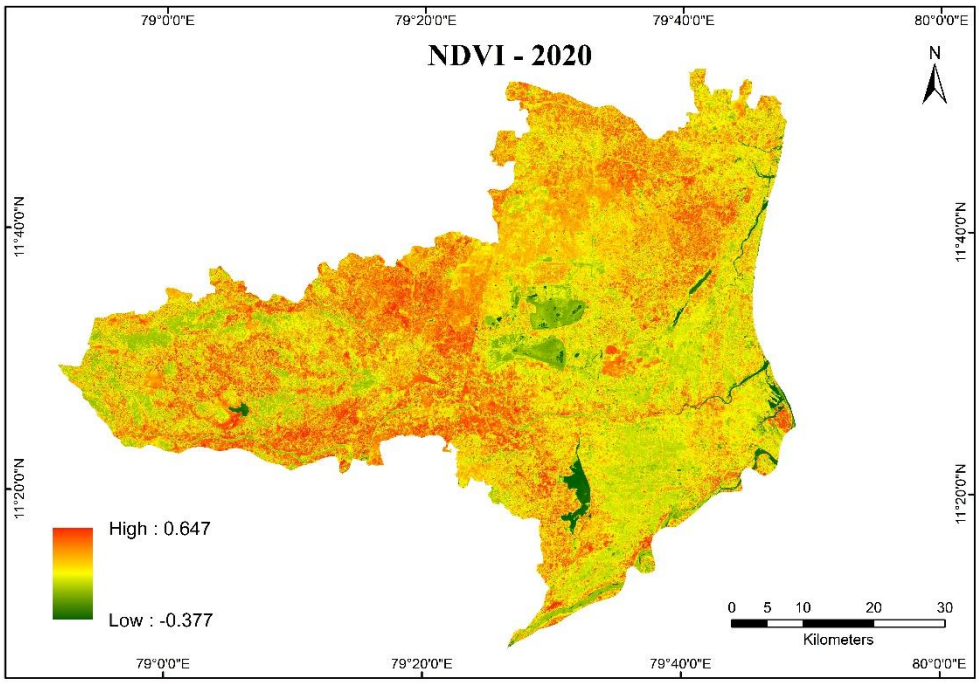

Figure 4 NDVI for the year 2020

LULC also mapped the study area for 2015, 2018 and 2020 using the same Landsat 8 data (Figure 5, 6,7). LULC mapping was carried out for the six classes :(i) water body, (ii) settlement land, (iii) wasteland, (iv) sparse vegetation, (v) moderate vegetation and (vi) dense vegetation. NDVI Threshold ranges were used for different land use classifications in 2015, 2018 and 2020 to identify the results. Table 1 shows the various threshold values.

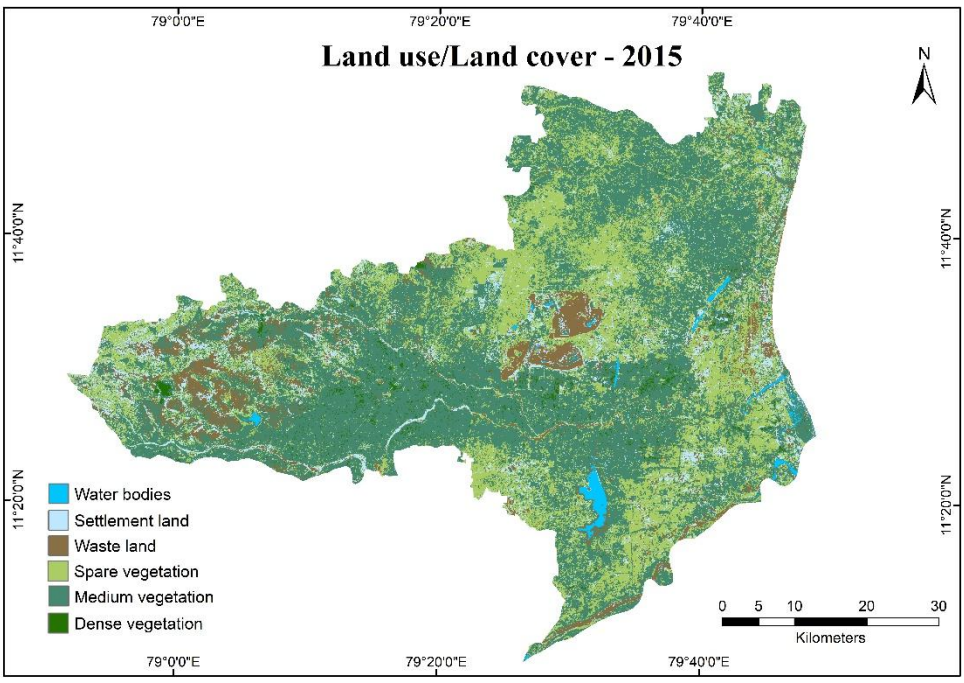

Figure 5 LULC for 2015

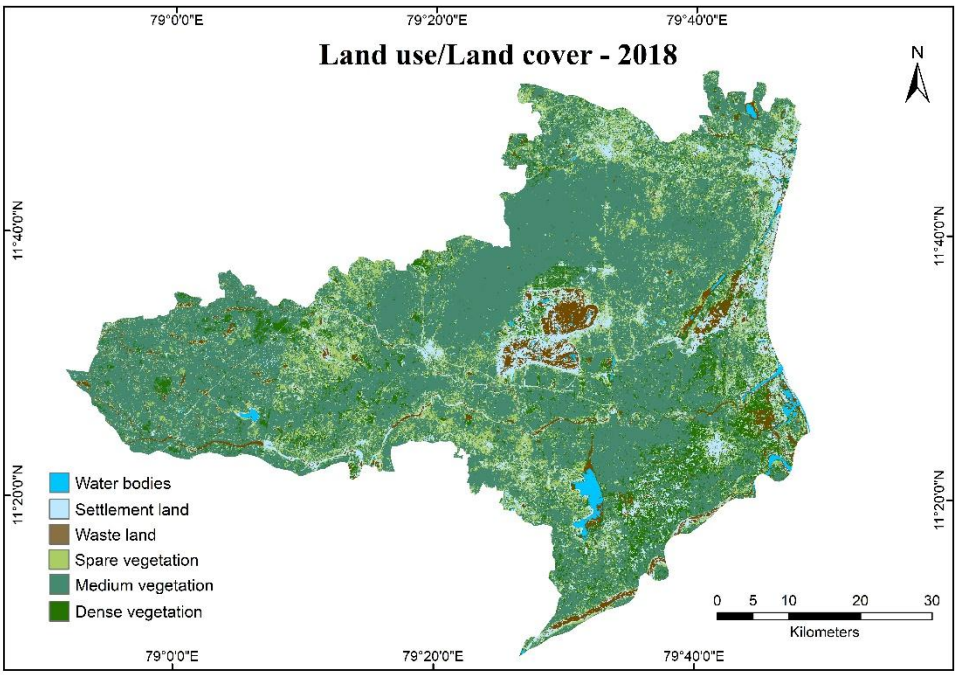

Figure 6 LULC for the year 2018

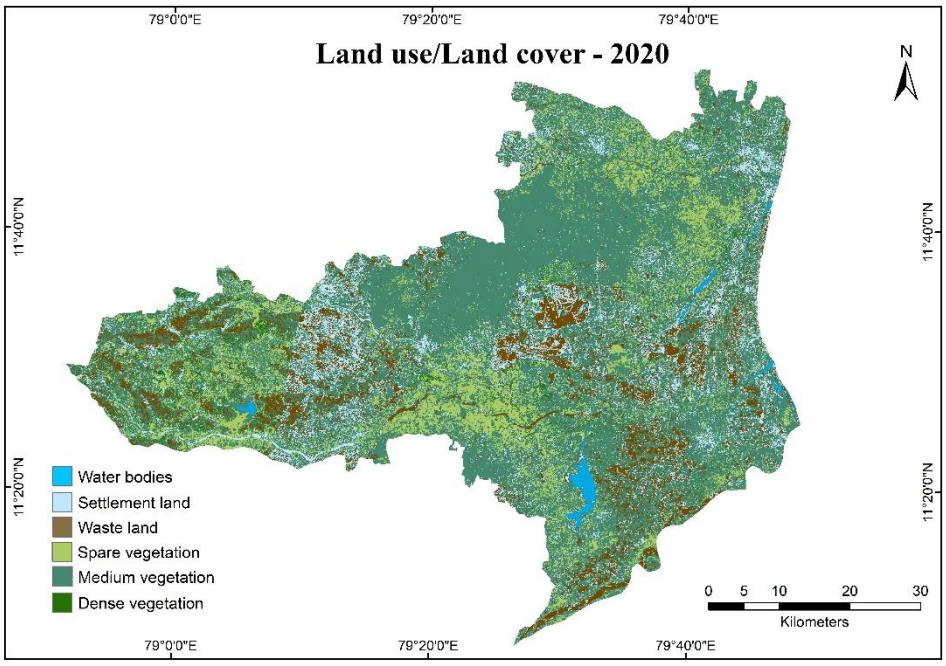

Figure 7 LULC for the year 2020

Table 1 NDVI Threshold range for Different land use classification in the year 2015, 2018 and 2020.

Land Use classification	**Thresholds (NDVI Values)**		
	2015	**2018**	**2020**

Water bodies	-0.432 - 0.01	-0.621 - 0.02	-0.781 - 0.06
Settlement land	0.03 to 0.12	0.04 to 0.14	0.03 to 0.09
Waste land	0.03 to 0.11	0.04 to 0.13	0.01 to 0.15
Spare vegetation	0.10 - 0.13	0.14 - 0.19	0.15 - 0.16
Moderate vegetation	0.24 to 0.26	0.19 to 0.22	0.22 to 0.23
Dense vegetation	0.27 to 0.60	0.23 to 0.53	0.20 to 0.49

The maps were created using the threshold values.
Figure 8,9,10 shows the NDVI threshold map of the study area

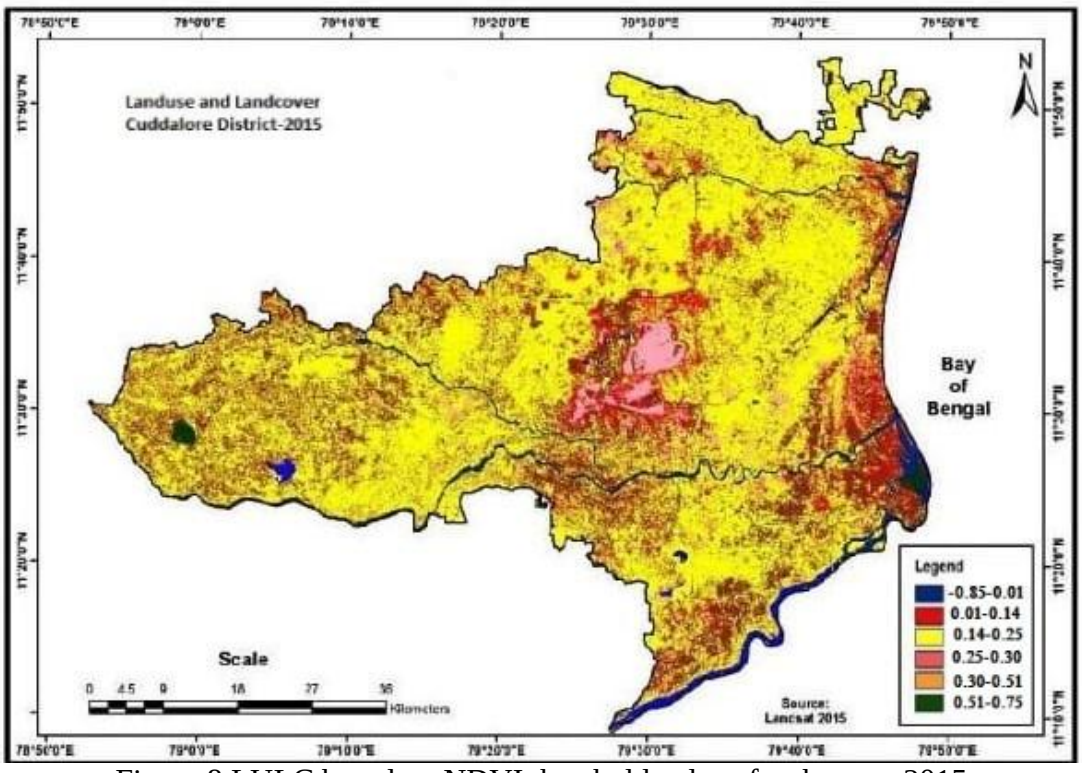

Figure 8 LULC based on NDVI threshold values for the year 2015

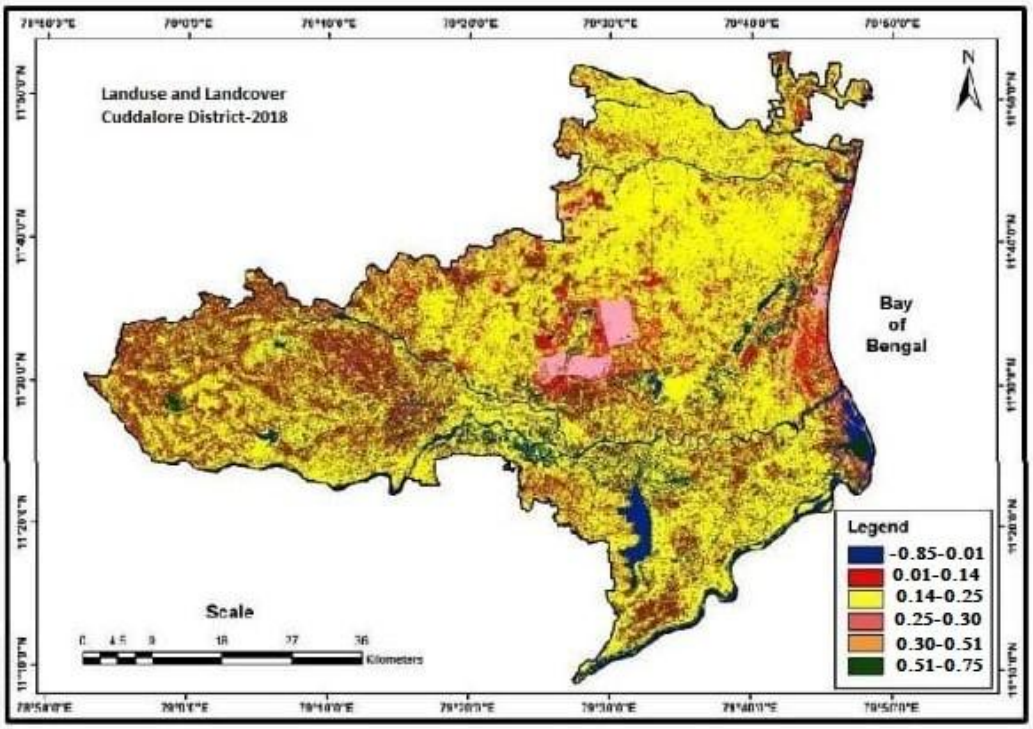

Figure 9 LULC based on NDVI threshold values for the year 2018

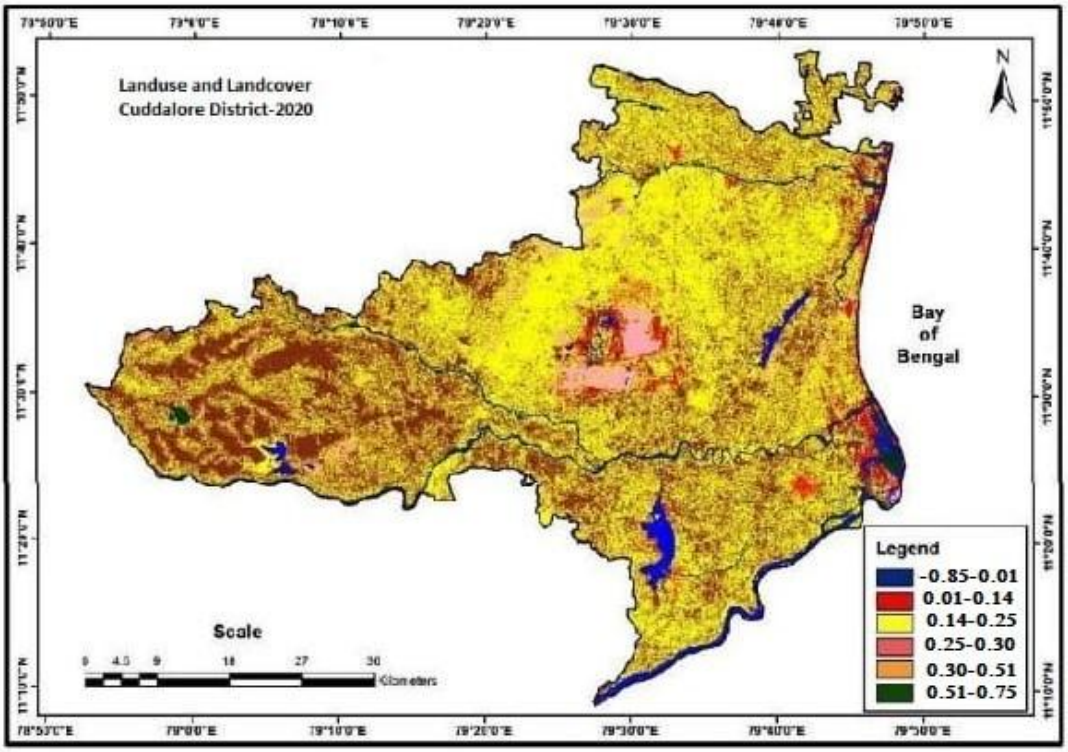

Figure 10 LULC based on NDVI threshold values for the year 2020

Land-surface types are not affected much by NDVI values (Raynolds *et al.*, 2008). The NDVI values depend on the presence of water vapour and aerosols as well as phenological response. Hence NDVI values are very sensitive to ecosystem conditions. Therefore, it is one of the

indicators of environmental change. Hence, NDVI base LULC classification is the better option for the study.

4.1 Estimation of Carbon Storage in Different Vegetation and Soils in Cuddalore:

Carbon storage in each place is critical for the ecosystem's stability. Carbon is generally stored in the form of biomass (biological material). Carbon dioxide is transformed into organic matter by green vegetation during the photosynthesis process. The carbon content of organic matter is held in vegetation for an extended time in various forms until it is released into the atmosphere by respiration, decomposition, or disturbance. Carbon is stored in significant quantities in woody biomass (roots, trunks, and branches) (Coomes *et al.*, 2012). The remainder eventually decomposes into organic matter in the form of floor litter and soils. Carbon storage changes in a particular area can be attributed to a range of anthropogenic and natural factors.

Carbon is extracted or released from the ecosystem when vegetation is harvested; forest land is cleared for other purposes such as agriculture or development or when the ecosystem is disturbed by wildfire, insects, or disease. Carbon storage can occur because of the natural regrowth of previously cleared agricultural land.

Carbon storage can also be increased through active tree planting and correct management procedures, which increase growth rate and, ultimately, in biomass amount (Fahey *et al.*, 2010). Carbon sequestered in each place is significant for a variety of reasons. The amount of carbon can determine the ecosystem of a specific location in the atmosphere, i.e., increasing or decreasing.

Carbon storage is inextricably linked to other critical ecological processes, such as the ecosystem's primary productivity (Dixon et al. 1994). Carbon dioxide is the most significant greenhouse gas emitted by human activity. Carbon sequestered by vegetation can help mitigate climate change. Carbon dioxide is removed from the atmosphere by green plants. As a result, green foliage can act as a net carbon sink, offsetting greenhouse gas emissions. Areas that emit more carbon than they store operate as net carbon sources, ultimately contributing to an increase in atmospheric carbon dioxide. The entire area was categorised into five LULC kinds in this study. The various LULC 40 contain varying amounts of biomass. It is critical to assess the carbon content of each LULC to determine the stability of the research area's ecosystem. As a result, the carbon storage capacity of the ecosystem has been selected by estimating the amount of carbon in each pool within the research region.

4.2 Calculation Of Soil Organic Matter:

To determine the carbon content of the soil, random samples were taken from the entire study area based on the LULC on the map. Soil samples were taken from a depth of 100cm below the ground surface. The soil samples were stored in an airtight container. The soil samples were taken to the soil lab for bulk density estimation. Containers were labelled according to their LULC type. The bulk density of the soil samples was determined and classified according to their LULC type. Settlement and wasteland bulk densities were determined to be between 1.2 and 1.4 g/cm3. The average thickness of 1.3g/cm3 is used for analysis. Similarly, for other LULC, estimates were made, and the average values were used in the study, as shown in Table 4.2.

Table 4.2 The Average Bulk Density of Soils in Different LULC

S No	Land use classification	Experimental bulk Density range g/cm3	Bulk Density g/cm3
1	Settlements and Wasteland	1.4 - 1.2	1.3
2	Sparse Vegetation	1.5 - 1.3	1.4
3	Moderate Vegetation	1.6 - 1.4	1.5
4	Dense Vegetation	1.5 - 1.7	1.6

The carbon content in t/ha for each LULC has been estimated by using the following equation:
SOC = [SOC] × BD × Depth × 10
Were,
SOC: soil organic Carbon (Mg/ha)
[SOC]: the concentration of soil organic carbon in each soil mass (g C/kg soil sample)
BD: bulk density the soil mass per sample volume (Mg/m3)
Depth: the depth of the soil sample (m)
The soil organic carbon concentration at a given sample is usually estimated using either dry combustion or the Walkley–Black method.
SOM = SOC / 1.7
Were
SOC: Soil Organic Carbon (SOC) content.

4.3 Calculation Of Dead Organic Matter:

Deadwood contains carbon in the form of decomposing organic materials. As a result, it is necessary to understand dead organic materials. To determine the amount of decomposing organic matter, a field survey was done to ascertain the height and diameter of the deadwood. Ten samples were measured in height and diameter. The average height and diameter of deadwood were estimated for various LULC and are shown in Table 4.3.

Table 4.3 The Average Height and Diameter of the Dead Wood in Different LULC

S No	Land use classification	Average height in cm	Average diameter in cm
1	Settlements and Wasteland	200	25
2	Sparse Vegetation	400	50
3	Moderate Vegetation	800	80
4	Dense Vegetation	1200	100

Knowing the height and diameter of deadwood, the whole dry organic matter in each plot has been estimated by using the following equation:

$$\boldsymbol{V = \frac{1}{3} \times \pi \times h \times (d^2)}$$

were,
V = volume of dead wood in cm3
h = height of dead wood in cm
d = diameter of dead wood in cm

$$\boldsymbol{dom = V \times \rho_{wood} \times 0.01}$$

were,
dom = dry organic matter in kg
V = volume of deadwood in cm3
ρ_{wood} = wood density (0.843 g/cm3)

The following equation has estimated the carbon pool (t/ha) in deadwood:

$$\boldsymbol{dom_c = dom \times 10^{-3} \times C_{fdom}}$$

were,
dom_c=carbon quantity in dry organic matter (t/ha)
dom =dry organic weight in kg
C_{fdom} = Fraction of Carbon in dry organic matter. It is assumed to be the same as biomass fraction, i.e., 47% of the dom.

4.4 Calculation For Four Carbon Pools Data:
The field survey was conducted to collect all the necessary data for preparing the database that would be used to compute the quantity of carbon sequestered or lost in the research area.

Table 4.4 Carbon Pools of Different Land Use Classification

Sl.no	**Land use classification**	**Soil Organic Matter (t/ha)**	**Dead Organic Matter (t/ha)**
1	Settlements and Wasteland	286	0.0518
2	Sparse Vegetation	308	0.4146
3	Moderate Vegetation	330	2.1232
4	Dense Vegetation	352	4.9763

4.5 Calculation Of Above-Ground Biomass And Below-Ground Biomass:
The AGC and BGC values were calculated using a tree and root biomass technique. Non-destructive biomass allometric equations for each mangrove species were preferred for biomass measurement. In the absence of an allometric equation for a given species, Komiyama et al. (2005) created common mangrove biomass allometric equations.

To calculate total mangrove biomass, he uses equations including tree and root biomass. In his equation, he included the wood density (kg/m3) of each mangrove species as an input to account for the variance in biomass among mangrove species.
During field data collecting, tree dbh (diameter at breast height), tree height, and species composition were all measured.
The tree is suitable for any stand with a diameter greater than 5 cm. A pole is a young stand with a dbh of between 5 and 49 cm, while a sapling is any stand with a height of at least 1.5 m. Each stand's above- and below-ground biomass was determined individually.
Aboveground Biomass= 0.251 ρ *D*BH $^{2.46}$
Dmax = 49 cm
Below ground Biomass = *0.199* ρ *0.899 D*BH $^{2.22}$
Dmax = 49 cm
Were
ρ: Wood density of the corresponding mangrove species = 0.843 g/cm^3
DBH: Diameter at breast height (cm)

4.6 Calculation of carbon sequestration in a tree
CO_2 is composed of one molecule of carbon and 2 molecules of Oxygen.
The atomic weight of carbon is 12.001115.
The atomic weight of Oxygen is 15.9994.
The weight of CO_2 is C+2*O=43.999915.
The ratio of CO_2 to C is 43.999915/12.001115=3.6663.
Therefore, to determine the weight of carbon dioxide sequestered in the tree, multiply the weight of carbon in the tree **by 3.6663 and divide the result by 10**

Table 4.5 Carbon sequestration of different DBH of the trees

DBH (cm)	**AGC(Kg)**	**BGC(Kg)**	**Total Carbon Storage (Kg)**	**Carbon Sequestration (Kg tree^{-1}year^{-1})**
5	11.1	6.08	17.18	6.30
10	61.02	28.33	89.35	32.76
15	165.46	69.69	235.14	86.21
20	335.76	131.98	467.74	171.49
25	581.34	216.60	798.02	292.58

30	910.37	324.67	1235.04	452.80
35	1130.17	457.15	1587.32	581.96
40	1847.43	614.90	2462.33	902.76
45	2468.33	798.66	3266.99	1197.77
49	3043.57	964.88	4008.45	1469.62

Table 4.6 Total Carbon Sequestration values

DBH (cm)	**Total Carbon Storage (Kg)**	**Carbon Sequestration (Kg tree^{-1}year^{-1})**
5-10	17.18 -89.35	6.30-32.76
10-15	89.35-235.14	32.76-86.21
15-20	235.14-467.74	86.21-171.49
20-25	467.74-798.02	171.49-292.58
25-30	798.02-1235.04	292.58- 452.80
30-35	1235.04-1587.32	452.80-452.80
35-40	1587.32-2462.33	581.96-581.96
40-45	2462.33-3266.99	902.76-902.76
45-49	3266.99-4008.45	1197.77-1469.62

From the above table, it is inferred that for the DBH of range 5 cm to 49 cm, the carbon sequestration is a minimum of 6.30 Kg tree-^{1}year^{-1} to a maximum of 1469.62 Kg tree-^{1}year^{-1}. From the field study, a tree's average carbon sequestration of around 522.43 kg is released annually.

5. CONCLUSION

The Landsat- 8 images were extracted from the https://www.usgs.gov/ USGS website at level 2 after correcting radiometric and georeferenced by using topo-sheets for generating LULC images by using ERDAS IMAGINE software. NDVI Threshold range for Different land use classifications such as Water bodies, Settlement and Wasteland, Spare vegetation, Moderate vegetation, and Dense vegetation for the years 2015, 2018 and 2020 were calculated and density vegetation LULC is mapped using GIS software for the respective years. To calculate Carbon sequestration, field data were collected from living trees, i.e., diameter at breast height, root shoot ratio, bulk density of soil and dead tree height and diameter. The estimated carbon pool is used to determine the carbon stock in the soil, above and below biomass. A maximum of 352 t/ha of Soil organic matter and 4.9763 t/ha of Dead organic matter for the dense vegetation was found in the soil, tested in the soil. It is concluded that the minimum and maximum of carbon sequestration are computed as 6.30 Kg tree-^{1}year^{-1} and 1469.62 Kg tree-^{1}year^{-1} respectively for the DBH of tree range from 5 cm to 49 cm. The field study shows that a tree per year releases average carbon sequestration of around 522.43 kg**.**

6. REFERENCE

[1] Aiazzi, B. *et al.* (2009) 'A comparison between global and context-adaptive pansharpening of multispectral images', *IEEE Geoscience and Remote Sensing Letters*, 6(2), pp. 302–306.
[2] Aran Castro A J *et al.* (2021) 'Mapping LULC changes of the coastal Kanyakumari district , Tamil Nadu , India Using Geospatial technology', *International journal of aquatic science*, 12(02), pp. 3419–3439.
[3] Coomes, D. A. *et al.* (2012) 'A general integrative framework for modelling woody biomass production and carbon sequestration rates in forests', *Journal of Ecology*, 100(1), pp. 42–64.
[4] Djomo, A. N. *et al.* (2010) 'Allometric equations for biomass estimations in Cameroon and pan moist tropical equations including biomass data from Africa', *Forest Ecology and Management*, 260(10), pp. 1873–1885.
[5] Fahey, T. J. *et al.* (2010) 'Forest carbon storage: ecology, management, and policy', *Frontiers in Ecology and the Environment*, 8(5), pp. 245–252.
[6] Giri, R. and Madla, V. R. (2017) 'Study and Evaluation of Carbon Sequestration using Remote Sending and GIS: A Review on Various Techniques', *International Journal of Civil Engineering and Technology*, 8(4), pp. 287–300.
[7] Horwath, W. (2007) 'Carbon cycling and formation of soil organic matter', in *Soil microbiology, ecology and biochemistry*. Elsevier, pp. 303–339.
[8] Köhl, M., Magnussen, S. and Marchetti, M. (2006) *Sampling methods, remote sensing and GIS multiresource forest inventory*. Springer.
[9] Kriegler, F. J. *et al.* (1969) 'Preprocessing transformations and their effects on multispectral recognition', in *Proceedings of the 6th international symposium on remote sensing of environment*.
[10] Liu, J. G. (2000) 'Evaluation of Landsat-7 ETM+ panchromatic band for image fusion with multispectral bands', *Natural Resources Research*, 9(4), pp. 269–276.
[11] Orr, F. M. (2004) 'Storage of carbon dioxide in geologic formations', *Journal of Petroleum Technology*, 56(09), pp. 90–97.
[12] Pagare N S *et al.* (2021) 'Mapping the wetlands of Mumbai and surrounding area using

Remotely sensed Sentinel-2b data', *Turkish online journal of qualitative inquiry*, 12(7), pp. 6964–6980.
[13] Pardo-Pascual, J. E. *et al.* (2012) 'Automatic extraction of shorelines from Landsat TM and ETM+ multi-temporal images with subpixel precision', *Remote Sensing of Environment*, 123, pp. 1–11.
[14] Peterson, C. L. and Hustrulid, T. (1998) 'Carbon cycle for rapeseed oil biodiesel fuels', *Biomass and bioenergy*, 14(2), pp. 91–101.
[15] Raynolds, M. K. *et al.* (2008) 'Relationship between satellite-derived land surface temperatures, arctic vegetation types, and NDVI', *Remote Sensing of Environment*, 112(4), pp. 1884–1894.
[16] Settle, J. J. and Briggs, S. A. (1987) 'Fast maximum likelihood classification of remotely-sensed imagery', *International Journal of Remote Sensing*. doi: 10.1080/01431168708948683.
[17] Tripathi, S. *et al.* (2010) 'Calculating carbon sequestration using remote sensing and GIS', *Geospatial world*, pp. 1–8.